Published in final edited form as:
*Cell Calcium*. 2013 April ; 53(4): 286–296. doi:10.1016/j.ceca.2013.01.002.

# LUMINAL $Ca^{2+}$ DEPLETION DURING THE UNFOLDED PROTEIN RESPONSE IN *Xenopus* OOCYTES: CAUSE AND CONSEQUENCE

**R. Madelaine Paredes**[a,1], **Mariana Bollo**[b], **Deborah Holstein**[a], and **James D. Lechleiter**[b,2]

[a]Department of Cellular and Structural Biology, University of Texas Health Science Center at San Antonio (UTHSCSA), San Antonio, Tx, USA

[b]Instituto de Investigación Médica Mercedes y Martín Ferreyra (INIMEC CONICET), Universidad Nacional de Córdoba, Córdoba, Argentina

## Abstract

The Endoplasmic Reticulum (ER) is a $Ca^{2+}$ storing organelle that plays a critical role in the synthesis, folding and post-translational modifications of many proteins. The ER enters into a condition of stress when the load of newly synthesized proteins exceeds its folding and processing capacity. This activates a signal transduction pathway called the Unfolded Protein Response (UPR) that attempts to restore homeostasis. The precise role of ER $Ca^{2+}$ in the initiation of the UPR has not been defined. Specifically, it has not been established whether ER $Ca^{2+}$ dysregulation is a cause or consequence of ER stress. Here, we report that partial depletion of ER $Ca^{2+}$ stores induces a significant induction of the UPR, and leads to the retention of a normally secreted protein Carboxypeptidase Y. Moreover, inhibition of protein glycosylation by tunicamycin rapidly induced an ER $Ca^{2+}$ leak into the cytosol. However, blockade of the translocon with emetine inhibited the tunicamycin-induced $Ca^{2+}$ release. Furthermore, emetine treatment blocked elF2α phosphorylation and reduced expression of the chaperone BiP. These findings suggest that $Ca^{2+}$ may be both a cause and a consequence of ER protein misfolding. Thus, it appears that ER $Ca^{2+}$ leak is a significant co-factor for the initiation of the UPR.

### Keywords

endoplasmic reticulum stress (ER stress); unfolded protein response (UPR); calcium signaling; protein misfolding; α subunit of eukaryotic translation initiation factor 2 (eIF2 α); thapsigargin (Tg); tunicamycin (Tn)

## 1. INTRODUCTION

The endoplasmic reticulum (ER) is an intracellular organelle that occupies about 10% of the total cell volume in most eukaryotic cells, which corresponds to more than 50% of the total



[2]Corresponding Author: James D. Lechleiter, Ph.D. 8403 Floyd Curl Drive, San Antonio, TX 78229-3900. Phone: 210-562-4043, Fax: 210-562-4146 Lechleiter@uthscsa.edu.
[1]Current address: Department of Psychiatry, University of Texas Health Science Center at San Antonio (UTHSCSA), San Antonio, TX, USA

cell membrane [1]. Protein and lipid synthesis, as well as post-translational modifications such as protein folding, sorting, and glycosylation, are some of the functions of the ER [2]. The ER co-ordinates these events and luminal $Ca^{2+}$ acts as a link between physiological status of the cell and the synthesis and processing of lipids and proteins. Consequently, it is critical to maintain $Ca^{2+}$ concentrations at sufficient levels for the proper functioning of the organelle [2–7]. If any of the ER functions is disrupted, the organelle enters into stress and a protective response known as the unfolded protein response (UPR) is triggered [3–6]. The UPR comprises three branches, which are initiated by inositol–requiring protein 1α (IREα), activating transcription factor 6 (ATF6) and (PKR)-like ER kinase (PERK) [8].

One of the earliest steps in this response is the attenuation of protein translation via PERK, which is an ER stress sensor that phosphorylates the α subunit of eukaryotic translation initiation factor 2α (eIF2α) [9]. Additional changes that promote long-term adaptation are transcriptional upregulation of ER chaperones including BiP, and molecules involved in the ER associated degradation (ERAD). If ER damage is persistent or excessive, cell death pathways are triggered [10].

Generally, the UPR is associated with luminal accumulation of misfolded proteins and ER $Ca^{2+}$ depletion [5]. $Ca^{2+}$ release (or loss) from the ER has been related with different diseases including Alzheimer's disease [11], Parkinson's Disease [12], prion-related disorders [13], HIV dementia [14] as well as Diabetes [15]. Interestingly, these disorders involve problems with folding and processing of proteins where the accumulation of large aggregates is thought to contribute to cellular damage that may accelerate the course of the disease. Moreover, many of these pathologies that involve accumulation of proteins have been associated with ER stress and the induction of UPR [16–18]. It is well established that $Ca^{2+}$ is a versatile second messenger involved in a broad variety of physio-pathological events [3]. However, it has not been determined the extent to which ER $Ca^{2+}$ plays a causative role in those protein folding disorders and whether ER $Ca^{2+}$ leak is a consequence of misfolded protein accumulation.

Moreover, the sensitivity of the ER to changes in luminal $Ca^{2+}$ has not been carefully investigated. Multiple groups have studied the physiological effects of fully depleting $Ca^{2+}$ from the ER stores in many different cell types using thapsigargin (Tg) treatment [19, 20]. Tg is a very specific and irreversible inhibitor of the Sarco Endoplasmic Reticulum Calcium ATPase (SERCA) [21]. SERCAs are a family of proteins responsible for transporting $Ca^{2+}$ from the cytosol into the lumen of the ER [22]. By inhibiting SERCA, refilling of $Ca^{2+}$ to the ER stores can no longer be achieved resulting in a slow release of this ion into the cytosol through leak channels [23]. Several research groups have proposed that a basal $Ca^{2+}$ leak occurs via the translocon [24–28]. The translocon is an aqueous pore that functions as a protein conducting channel that spans the ER lipid bilayer [29] through which newly synthesized secretory proteins are translocated into the lumen of ER [30]. Recently, it has been demonstrated at cellular level, that BiP and $Ca^{2+}$-Calmodulin facilitate the translocon channel gating from the open to the closed state [31, 32].

Studies to date have utilized Tg to examine the impact of $Ca^{2+}$ on ER stress, but at concentrations known to cause total $Ca^{2+}$ depletion. This is very detrimental to cells and eventually leads to apoptosis [33]. Therefore one of the goals of this study was to determine the consequences of a more physiologically relevant, partial luminal $Ca^{2+}$ depletion on ER stress, protein folding and the UPR. Our strategy was to partially deplete the ER $Ca^{2+}$ stores of *Xenopus* oocytes and monitor the induction of the UPR as well as the ER retention and accumulation of a normally secreted protein Carboxypeptidase Y (CPY-wt) [34, 35]. The second goal was to determine the impact of protein misfolding on ER $Ca^{2+}$ release and the initiation of the UPR. For this, we induced protein misfolding by overexpression of the

mutant misfolded protein ($CPY_{G255R}$) or by inhibition of protein glycosylation with tunicamucin (Tn) and monitored ER $Ca^{2+}$ levels and induction of the UPR.

## 2. MATERIAL AND METHOS

### 2.1 Construction of expression vectors

Wild-type Carboxypeptidase Y (CPY-wt) was achieved by PCR amplification from a DNA library of *Saccharomyces cerevisiae* obtained as a gift of Dr. McAlister-Henn (Department of Biochemistry UTHSCSA). CPY-wt was amplified using the forward primer with sequence 5'- ATC GCG **CCC GGG A**TG AAA GCA TTC ACC AGT TTA CTA -3' introducing the SmaI site (**in bold**) and reverse primer 5'- ATC G**AA GCT T**TT ATA AGG AGA AAC CAC CGT GGA TC-3' introducing the HinDIII site (**in bold**). The mutant $CPY_{G255R}$ was generated by site directed mutagenesis using the forward primer with sequence 5'- CAA GAT TTC CAC ATC GCT ***A***GG GAA TCC TAC GCC GGC CAT TAC-3' and it's complementary reverse primer 5'- GTA ATG GCC GGC GTA GGA TTC CC***T*** AGC GAT GTG GAA ATC TTG -3' introducing mutation G255R (**in bold and *italic***). The primers used in the amplification of CPY-wt and mutant $CPY_{G255R}$ were purchased from Invitrogen Corporation (Carlsbad, California). Wild-type Carboxypeptidase Y and mutant $CPY_{G255R}$ were subcloned between the 5' and 3' untranslated regions of *Xenopus* laevis β-globin vector (pHN) as described previously [4] in between the SmaI and HinDIII restriction sites.

Fluorescent proteins mStrawberry (mStr) and mCyan fluorescent protein (mCFP) were obtained as a gift from Dr. Roger Tsien (University of California / Howard Hughes Medical Institute). Fusion construct CPY-wt-mStr was generated by PCR amplification with a forward primer (called 5' SmaI-CPY) with sequence 5'-ATC GCG **CCC GGG** ATG AAA GCA TTC ACC AGT TTA CTA -3' introducing the SmaI site (**in bold**) and a reverse primer (called 3'mstrawberry-CPY) with sequence 5'-***CTC CTC GCC CTT GCT CAC CAT*** TAA GGA GAA ACC ACC GTG GAT C-3' introducing part of m-strawberry sequence (**in bold and *italic***). m-strawberry was amplified using pRsetB-mstrawbrerry as template and a forward primer (called 5'CPY-mstrawberry) with sequence 5'-***GAT CCA CGG TGG TTT CTC CTT A***AT GGT GAG CAA GGG CGA GGA G-3' introducing part of CPY sequence (**in bold and *italic***) and a reverse primer (called 3'HinDIII-mstrawberry) with sequence 5'-ATC G**AA GCT T**TT ACT TGT ACA GCT CGT CCA TG- 3' introducing the HinDIII site (**in bold**).

Similarly, fusion construct $CPY_{G255R}$-CFP was generated using a forward primer (called 5'CPY-mstrawberry, described above) and a reverse primer called 3' HindIII-mCFP with sequence ATC G**AA GCT T**TT AAC ACT GGC GGC CGT TAC TAG introducing the HinDIII site (**in bold**). The use of primers 5'CPY-mstrawberry and 3'mstrawberry-CPY on the amplification of mCFP was possible because mStr and mCFP share identical sequence on the first 21 base pairs.

Fusion constructs CPY-wt-mStr and $CPY_{G255R}$-mCFP were subcloned between the SmaI and HindIII restriction sites of *Xenopus* laevis β-globin vector (pHN) as described previously [4].

Fluorescent construct pCDNA3-D1ER was also obtained as a kind gift from Dr. Roger Tsien (University of California / Howard Hughes Medical Institute). PCR amplification of D1ER was performed by using the forward primer 5'BamH1 D1ER based on Tsien's sequence 5' ATCG **GGATCC** ATG CTG CTG CCC GTC CCC CTG- 3', introducing BamHI site (**in bold**) and 3' EcoRI-D1ER 5'-ATCG **GAATTC** TTA CAG CTC GTC CTT GCC GAG AGT GAT CCC -3' introducing EcoRI site (**in bold**). Purification of PCR

product was immediately followed by subclonig into the *Xenopus* expression vector pHNb. Restriction enzymes were obtained from Invitrogen Corporation (Carlsbad, California). Sequencing of all cDNA constructs was performed at the Nucleic Acids core facility at UTHSCSA.

### 2.2 *In vitro* transcription

CPY-wt-mStr, mutant $CPY_{G255R}$-CFP and pHNb-D1ER mRNA were prepared as described previously [36].

### 2.3 *Xenopus laevis* oocyte microinjection

Manually defolliculated *Xenopus laevis* oocytes stages VI were incubated overnight in MBS at 18°C. MBS medium contains 10 mM HEPES pH 7.5, 88mM NaCl, 10 mM KCl, 0.41 mM $CaCl_2$, 0.33 mM $Ca(NO_3)_2$, 0.82 mM $MgSO_4$, 2.4 mM $NaHCO_3$, all chemicals obtained from Sigma-Aldrich (St. Louis, Missouri). One day after defoliculation, oocytes were microinjected with a bolus of 50 nl of mRNA (0.7 μg/μl) using an standard positive pressure injector (Drummond Scientific, Broomall, Pennsylvania) as described by Roderick et.al. [37]. In brief, glass capillaries (6 cm) with tip diameters of ~10 μm (Drummond Scientific, Broomall, Pennsylvania) were prepared with a horizontal puller (Sutter Instruments, Novato, California) and the tip was broken against a barrier under a light microscope (Micro Forge, MF-900, Narishige). The glass needle was filled with mineral oil by using 1 ml syringe with $25_{1/2}$ size needles. 3 μl of mRNA solution was pipetted onto parafilm and a glass microelectrode was backfilled using a Nanoject microinjector (Drummond Scientific, Broomall, Pennsylvania). Microinjected oocytes were incubated for 3–5 days in OR-3 medium that was changed daily.

### 2.4 Confocal imaging of luminal $Ca^{2+}$ depletion via cytosolic $Ca^{2+}$ release in *Xenopus* oocytes

Thapsigargin (Tg) was prepared as 10mM stock (Sigma-Aldrich, St. Louis, Missouri). Oocytes were maintained in OR-3 medium plus Tg at a specific concentration (50 nM, 100 nM, 150 nM, 200 nM, 500 nM and 1 μM) for 24 or 48 hours. Vehicle control oocytes were maintained in OR-3 medium in the presence of DMSO at the same concentrations used in corresponding Tg treated groups. A subgroup of oocytes was left untreated and used as control.

On the imaging day, oocytes medium was replaced with fresh OR-3 medium. Then each oocyte to be used in confocal imaging was microinjected with 50 nl (50 μM final) of the $Ca^{2+}$ indicator dye fluo-4 pentapotassium salt (Invitrogen Corporation, Carlsbad, California), prepared in 200 mM pyruvate-malate (10 mM final in the oocyte). During injection and incubation with fluo-4 oocytes were placed in low $Ca^{2+}$ recording medium containing 96 mM NaCl, 2 mM KCl, 1 mM MgCl2, 5 mM HEPES Na (Sigma-Aldrich, St. Louis, Missouri). After 40 minutes incubation, individual oocytes were placed on the stage of a Nikon Eclipse TE 300 microscope with a 10× N.A. 0.3 air lens. Frames were collected every 2 seconds and after 20 frames (about 1 minute of recording), 6 μM $IP_3$ was microinjected (300 nM final) to stimulate luminal $Ca^{2+}$ release. Total recording was about 6 minutes for each oocyte (180 frames). Fluo-4 was excited at a wavelength of 488 nm, and emitted fluorescence was collected via a 510 nm filter, using a photomultiplier (PMT). The fluorescence intensity of the $Ca^{2+}$ indicator was analyzed using ImageJ (NIH) software and plotted as the change in fluorescence ($\Delta F/F = (F-Frest)/Frest$) over time. We measured both the peak fluorescence as well as the integrated area under the $\Delta F/F$ curve. Fluorescent images were acquired every two seconds. The area under the curve was calculated in an excel spreadsheet by adding the height ($\Delta F/F$, unitless) at each 2 second time point for 4

minutes. The integrated area roughly corresponds to the total amount of $Ca^{2+}$ released over this four-minute period (240 seconds).

### 2.5 Confocal Imaging of protein retention in the Endoplasmic Reticulum (ER)

Oocytes microinjected with a combination of mRNA of CPY-wt-Str and $CPY_{G255R}$-CFP (30 ng total) were maintained in OR-3 medium and incubated at 18 °C for protein expression. After 24 hours, oocytes were left untreated (control) or treated with 50 or 100 nM Tg and incubated at 18 °C for 24 or 48 hours, at which times they were confocaly imaged.

Protein folding in the ER was imaged using a Zeiss LSM510 inverted confocal microscope. The target imaging location was determined by focusing on the ER region (abut 10–20 μm of the surface of the oocyte) using a 63× objective N.A. 1.4 oil immersion objective. In this region, very distinguishable ER like structures were found as described by [38]. Images were collected sequentially in stacks of 10 slices with 1 μm in between using the CFP channel (458) corresponding to an Argon Laser and Str channel (543) corresponding to a Helium-Neon Laser.

ImageJ softare (NIH) was used for the initial analysis of the acquired images showing ER structures. Later, images were analyzed with the Open Lab software (Improvision, Lexington, MA) by obtaining fluorescence intensity values of selected regions of interest (ROI's) from the ER like structures. An average of 20 ROI's per image were selected from both CFP and Str images.

### 2.6 Western Blots

After treatment, oocytes were frozen in dry ice and maintained at −80 °C until preparation for western blots as described in Li. Y. 2004 [4]. Microsomal and Cytosolic fractions were isolated for analysis. In brief, oocytes were homogenized in Lysis buffer using a pellet pestle attached to a motorized homogenizer. Lysis buffer was prepared as described previously [37] containing 15 mM Tris HCl, pH7.6, 150 mM NaCl, 1% TritonX 100, 1mM EDTA supplemented with phosphatase and protease inhibitors (Sigma-Aldrich Sigma-Aldrich, St. Louis, Missouri). The nuclei debris fraction was removed by centrifugation at 4500 g for 15 minutes. The resulting supernatant was centrifugated at 120,000g for 30 min at 4°C to obtain the cytosolic fraction (supernatant) and the microsomal pellet, which was then resuspended in 30 μl of solubilization buffer (10 mM Tris HCl, pH7.6, 140 mM NaCl, 1% Triton X-100, 1% SDS) supplemented with phosphatase and protease inhibitors.

P-eIF2α was detected with an antibody from Assay Designs (Ann Arbor, Michigan). Actin was used for normalization with an antibody from Millipore (Temecula, California). Intensities of P-elF2α and actin bands were analyzed by Image J. The respective ratios (P-elF2α/actin) were averaged and reported as mean ± SEM. All values represent the means of at least 3 independent experiments.

### 2.7 Induction of ER stress with compounds that affect protein folding

Tunicamycin (Tn) (Sigma-Aldrich, St. Louis, Missouri) was prepared as 5 mg/ml in warm methanol and injected into oocytes for a final concentration of 2.5 μg/ml. Incubation time varied depending on the experiment.

### 2.8 Cytosolic $Ca^{2+}$ measurements after tunicamycin treatment and inhibition of translocon

*Xenopus* oocytes were treated with 2.5 μg/ml Tn (or methanol vehicle) for 1.30 hours in low $Ca^{2+}$ OR-3 medium, which contains OR-3 medium and 1.26 mM EGTA for a final $Ca^{2+}$ concentration of 7.6 μM. Oocytes were then injected with 50 μM of the $Ca^{2+}$ indicator dye

fluo-4 (Invitrogen-Molecular Probes, Eugene, OR). In order to block a possible ER $Ca^{2+}$ leak through the translocon, emetine was used at 1μM final concentration (Sigma-Aldrich, St. Louis, Missouri). After a 30 minutes incubation period with fluo-4, individual oocytes were imaged by confocal microscopy using a TE 200 Nikon inverted microscope with a 10× lens (N.A. 0.3 Air). Images were collected every 10 seconds for a total of 30 images (5 minutes of recording) per oocyte using a 488 nm excitation laser with a 510 nm emission filter. Fluorescense intensity values were obtained from each image and plotted as the change in fluorescence (ΔF/F) during the time of recording.

### 2.9 Confocal Imaging of D1ER construct

The $Ca^{2+}$ indicator D1ER was generated by Dr. Roger Tsien's laboratory [39]. Confocal imaging of D1ER injected oocytes was performed using an inverted IX-81 Olympus microscope configured with an Olympus FV1000 confocal scanning system. Images of the ER were collected with the UPLANAPO 60 X objective (N.A. 1.42 Oil). A lambda scan was performed to determine the emission spectrum of ECFP and citrine, by exciting D1ER from injected oocytes with a 458 laser. Emission was collected in a sequence of a 10 nm bandwidth at 5nm intervals (step size) over a range of 460 nm to 550 nm. Therefore 17 images were obtained from the lambda scan of each oocyte. Then, the best quality image from each oocyte was collected from ECFP and citrine. Oocytes were individually imaged for ECFP detection using a 458 excitation laser and for Cytrine with a 515 excitation laser.

### 2.10 Imaging analysis of D1ER

For each oocyte, fluorescence intensity values were obtained and corrected for autofluorescence and for CFP bleed through from the ECFP channel into the citrine channel. After both corrections were performed for each oocyte, an emission ratio of citrine/CFP (also referred as YFP/CFP) was calculated and values were averaged from oocytes from the same cohort.

### 2.11 $Ca^{2+}$ Imaging Analysis

$Ca^{2+}$ Imaging analysis was performed using the program ImageJ (Image Processing and Analysis in Java) designed by the U. S. National Institutes of Health and available to the public at http://rsbweb.nih.gov/ij/

### 2.12 Statistical analysis

Statistical significance was determined by using ANOVA. Significance level was accepted at $P < 0.05$.

## 3. RESULTS

### 3.1 Low thapsigargin concentrations partially deplete luminal $Ca^{2+}$

It is well established that high concentrations of Tg can totally deplete ER $Ca^{2+}$ stores [20, 21, 40]. However, the limited range of Tg concentrations at which $Ca^{2+}$ stores are only partially depleted is dependent on the cell type. In this series of experiments, our goal was to establish a protocol for partial depletion of the ER $Ca^{2+}$ stores in *Xenopus* oocyes. Oocytes were incubated for 24 or 48 hours with Tg at different concentrations (50 nM, 100 nM and 150 nM) or with vehicle at corresponding concentrations of DMSO (0.0005%, 0.001% and 0.00150%). The level of ER $Ca^{2+}$ was indirectly estimated by measuring the magnitude of $Ca^{2+}$ release induced by injection of inositol 1,4,5 trisphosphate ($IP_3$). Oocytes were injected with the $Ca^{2+}$ indicator dye fluo-4 and imaged with confocal microscopy to record an $IP_3$-stimulated $Ca^{2+}$ response (Figure 1A, 1B). Data obtained from these experiments were analyzed two ways to measure the effect of each Tg concentration and treatment period on

the releasable $Ca^{2+}$ pool. First, by measuring the peak of change in fluorescence from resting levels ($\Delta F/F$) during the time of recording (Figure 1C and 1D, top). And second by integrating the area under the $\Delta F/F$ curve over a 4 minutes period to estimate the total amount of $Ca^{2+}$ released during the time of recording (Figure 1C and 1D, bottom).

Both analyses indicated that after 24 hours of treatment with 50 nM Tg, there was no significant decrease in the magnitude of releasable $Ca^{2+}$ from the ER as compared to control oocytes (untreated or treated with vehicle) (Figure 1C). A suggestive trend is apparent, but not statistically significant. However, after 48 hours of treatment with this concentration of Tg, a significant decrease in the magnitude of the $IP_3$-releasable $Ca^{2+}$ from the ER stores was observed (Figure 1D, ANOVA $p< 0.05$). Treatment of oocytes with higher doses of Tg (100 nM) for 24 or 48 hours resulted in a smaller $Ca^{2+}$ response after $IP_3$ stimulation when compared to untreated or vehicle treated controls (ANOVA,*$p<0.05$, **$p<0.001$). Treatment with Tg concentrations higher than 150 resulted in total store depletion. These results suggest that partial depletion of $Ca^{2+}$ from the ER stores in *Xenopus* oocytes can be achieved with both 50 nM and 100 nM Tg treatments for 48 hours.

### 3.2 Low thapsigargin treatment induces the UPR

Several reports have indicated that cells treated with concentrations of Tg that totally deplete the ER $Ca^{2+}$ stores were able to induce ER stress and the UPR [33, 41–43]. To test the effects of partial ER $Ca^{2+}$ depletion on the induction of the UPR, a parallel group of oocytes were treated with the same concentrations of Tg (50 nM, 100 nM, and 150 nM) or with vehicle (DMSO) at the corresponding concentrations (0.0005%, 0.001% and 0.00150%). These oocytes were snap frozen and their cytosolic protein was extracted for western blot analysis of the UPR as indicated by phosphorylation of the eIF2α [9, 44, 45] and normalized with actin (for explanation see supplementary Figure 3). We observed that treatment of *Xenopus* oocytes with 50 nM Tg for 24 hours induced ER stress as seen by a significant increase in the phosphorylation of eIF2α compared to its vehicle control (Figure 2A and 2B). This effect was even more pronounced when oocytes were treated for 48 hours with Tg at 50 nM, 100 nM and 150 nM (Figure 2C and 2D). At this time point, there was an increase in phosphorylated elF2α for all groups treated with Tg that was significantly different from their controls (ANOVA, $P<0.05$). These results indicate that treatment of *Xenopus* oocytes for 48 hours with concentrations of Tg that partially deplete $Ca^{2+}$ from the ER stores (50 – 100 nM) also induce the UPR.

### 3.3 Expression of either CPY-wt-Str or Mutant $CPY_{G255R}$-CFP does not induce ER stress on *Xenopus* oocytes

Injections of a low concentration of mRNA may give rise to very low or undetectable levels of protein expression while high concentrations of mRNA could overwhelm the ER protein synthesis machinery and induce ER stress. Previous expression studies in oocytes were usually performed in a range of 1 – 30 ng of mRNA injected per oocyte [46]. To determine which mRNA concentrations were optimal for CPY expression but did not induce ER stress, we injected oocytes with 5 ng, 15 ng, and 30 ng of mRNA, for CPY-wt-Str, $CPY_{G255R}$-CFP and a combination of CPY-wt-Str with $CPY_{G255R}$-CFP (supplementary Figure 1). ER stress was assayed by western blot analysis of phosphorylated-elF2α (P-eIF2α) and normalized with actin as described above. We found that P-eIF2α immunoreactivity was not induced at any of the RNA concentrations used (supplementary Figure 1), demonstrating that these conditions of mRNA injections could be used without inducing ER stress due to protein expression.

### 3.4 Wild type CPY-Str translocation is disrupted by low levels of Tg treatment, while luminal retention of the mutant protein $CPY_{G255R}$-CFP is not affected

One of the goals of this study was to determine whether partial ER $Ca^{2+}$ depletion affected protein processing of a normally secreted protein. We demonstrated above that low levels of Tg partially depleted ER $Ca^{2+}$. Here, we used Tg concentrations to determine if folding and processing of a single protein, either wild type protein (CPY-wt-Str) or its mutant ($CPY_{G255R}$-CFP), were differentially affected by low luminal $Ca^{2+}$. Oocytes were simultaneously microinjected with mRNAs for both CPY-wt-Str and $CPY_{G255R}$-CFP (15 ng each). Injected oocytes were then treated with either 50 or 100 nM Tg, for 24 and 48 hours, and compared to non-treated controls. Induction of the UPR was monitored by western blot analysis of the phosphorylation of eIF2α (Figure 3).

As observed in supplementary Figure 1, non-treated oocytes injected with a combination of both mRNAs (control) did not increase P-eIF2α immunoreactivity when compared to non-injected (NI) controls (Figure 3A and 3B first two bars). After 24 hours of either 50 or 100 nM Tg treatment, P-eIF2α immunoreactivity was slightly, but not significantly increased. However, after 48 hours of Tg treatment, we observed a significant increase in P-eIF2α immunoreactivity compared to controls (untreated or non-injected oocytes) (ANOVA, $p<0.01$) (Figure 3C and 3D). To test whether partial $Ca^{2+}$ depletion and induction of the UPR by Tg affected protein folding and processing, we performed confocal imaging of the fluorescently tagged CPY wild type (CPY-wt-Str) and mutant ($CPY_{G255R}$-CFP) proteins. As expected, we observed that the misfolded protein $CPY_{G255R}$-CFP, was synthesized in the ER and remained in this organelle, regardless of the depletion of $Ca^{2+}$ or treatment with DMSO vehicle (Figure 4). This spatial distribution of the protein expression was observed for oocytes that were treated with Tg for either 24 or 48 hours (Figure 4B and 4E). On the other hand, when oocytes expressing the normally secreted protein CPY-wt-Str were subjected to treatment with low doses of Tg (50 nM and 100 nM), we observed a significant increase in protein fluorescence after 48 hours, indicating that it had been retained in the ER (Figure 5E compared to 5B). We concluded from these experiments that partial $Ca^{2+}$ depletion of the ER was sufficient to cause protein misfolding and accumulation in the ER, which in turn triggers a UPR.

### 3.5 ER $Ca^{2+}$ content is not significantly affected by expression of a mutant protein, $CPY_{G255R}$, that misfolds in the ER

Data presented above indicate that partial luminal $Ca^{2+}$ depletion induces protein misfolding and accumulation of the normally secreted protein carboxypeptidase Y (CPY-wt) in the ER. Our next question was to determine if misfolding and accumulation of proteins in the ER affected luminal $Ca^{2+}$ levels. To accomplish this, we chose to utilize the ER targeted $Ca^{2+}$ indicator D1ER [39]. The advantage of using this specific probe is that it's $Ca^{2+}$ affinity is relatively low (~69 μM) and doesn't saturate in the ER. Confocal images were collected from oocytes expressing D1ER to determine if the probe was properly targeted and functioning. When D1ER expressing oocytes were treated with Tg (100 nM), a significant drop in acceptor fluorescence (~540 nm) was observed (supplementary Figure 2E, F compared to supplementary Figure 2B, C).

In order to test whether misfolded proteins induced ER $Ca^{2+}$ release, we coexpressed D1ER with CPY-wt or with the mutant $CPY_{G255R}$ and examined the impact on ER $Ca^{2+}$ levels 48 hours later. Fluorescent measurements of D1ER (YFP/CFP emission ratio) indicated that there was no significant difference between D1ER alone the mutant $CPY_{G255R}$. Similarly, co-expression of D1ER with CPY-wt did not affect ER $Ca^{2+}$ concentration. Comparison of these results with oocytes expressing D1ER alone, but treated with Tg, confirmed that we could detect a small decrease in luminal $Ca^{2+}$ levels in the ER for oocytes treated with 50

nM and 100 nM Tg (ANOVA, $p < 0.05$) (Figure 6C). Moreover, ER $Ca^{2+}$ levels after treatment of oocytes with Tn for 2 hours is comparable with 50 nM Tg treatment of 24 hours (Figure 6 D). We concluded from these results that any change in the level of ER $Ca^{2+}$ induced by expression and accumulation of the misfolded protein $CPY_{G255R}$ was, if present, too small to be detected with the D1ER $Ca^{2+}$ indicator.

### 3.6 $CPY_{G255R}$ expression does not induce ER stress

A control experiment was designed to test whether D1ER expression by itself induced the UPR. Western blot analysis of the ER stress indicator P-eIF2α (normalized by actin) showed no increase in immunoreactivity in oocytes expressing D1ER when compared to control oocytes (Figure 6A). In addition, co-expression of D1ER with CPY-wt or the mutant $CPY_{G255R}$ did not increase the levels of P-eIF2a/actin either. The only condition in which ER stress was increased was when oocytes were treated with 100 nM Tg, which was significantly different when compared to control oocytes (ANOVA, $P < 0.05$) (Figure 6A and 6B). Consequently, we concluded that expression of the misfolded protein $CPY_{G255R}$, under this condition, was not sufficient to induce ER stress.

### 3.7 $Ca^{2+}$ leak via the translocon activates the UPR

As we previously reported, treatment of *Xenopus* oocytes with tunicamycin (Tn), an inhibitor of protein glycosylation, results in small but significant increases in cytosolic $Ca^{2+}$ [47] (Figure 7A, left). Recent work from other groups has suggested that the translocon itself may be a site of $Ca^{2+}$ leak under ER stress conditions [48]. To test whether this $Ca^{2+}$ leak affected the UPR, we pre-treated one group of oocytes with the translocon inhibitor emetine and another group with emetine plus Tn. We found that emetine treatment significantly inhibited the Tn-induced increase in cytosolic $Ca^{2+}$ (Figure 7A). Cytosolic $Ca^{2+}$ levels in control oocytes were not affected by treatment with vehicle alone. Under these conditions, we measured the effect of emetine treatment on phosphorylation of elF2α. Remarkably, emetine inhibition of the translocon not only blocked the $Ca^{2+}$ leak induced by Tn, but abrogated the increase in P-eIF2α (Figure 7 B, C, right). We also tested whether a different ER stress marker, the chaperone BiP was also affected by Tn and emetine treatment (Figure 7 D-E). We found that emetine significantly reduced BiP expression induced by Tn. Based on these data, we suggest that $Ca^{2+}$ released via the translocon, as a consequence of protein misfolding, is a critical signal for the initiation of the UPR.

## 4. DISCUSSION

The first goal of this study was to evaluate the impact of partial ER $Ca^{2+}$ depletion on protein processing and the UPR. We found that partial $Ca^{2+}$ depletion was sufficient to induce the UPR and to cause ER retention and accumulation of a model protein CPY-wt, that would otherwise be normally secreted under resting conditions. Second, we wanted to determine the effect of $Ca^{2+}$ leak via the translocon during the early phase of the UPR.

Several early studies reported that total $Ca^{2+}$ depletion significantly affects protein processing and secretion of glycoproteins [20, 40]. Our work goes one step further and suggests for the first time that partial $Ca^{2+}$ depletion affects the protein processing of a secreted single glycoprotein. First, to establish the conditions that induce partial ER $Ca^{2+}$ depletion and UPR, we carefully performed dose-response curves. As ER stress indicator we used phosphorylation of eIF2α due to its ability to remain active after mild and prolonged ER stress. By contrast the responses mediated by IRE1 and ATF6 sensors quickly attenuate within hours in spite of persistence of stress [49]. Although eIF2α phosphorylation could be transient [50, 51], this is related with a severe and acute ER stress. For example, Koumenis et. al. found that at least in HeLa cells the kinetics of eIF2α phosphorylation are dependent

on the oxygen concentration. For instance, under anoxic conditions, the phosphorylation of eIF2α is transient, while it remains constant under mild hypoxia [52].

The sensitivity of the ER protein-folding environment to changes in $Ca^{2+}$ also implies that small disruptions in $Ca^{2+}$ homeostasis could be a critical factor in human pathologies. Several diseases associated with a disruption of ER $Ca^{2+}$ are known to be associated with ER stress. Examples include disruption of ER $Ca^{2+}$ permeability in animal models associated with Alzheimer's [53]; increased ER $Ca^{2+}$ release induced by acute hypoxia in primary cultured astrocytes [54]; disruption of SERCA2b expression leading to a decreased ER $Ca^{2+}$ levels in a mouse model of obesity and diabetes [55] and increased ER stress levels in liver and adipose tissue [56]. Similar findings have been reported in other diseases as well [13, 57]. However, it has not been established in any of these diseases whether the underlying disruption of protein folding/processing machinery of the ER can be attributed to partial $Ca^{2+}$ depletion within the ER.

Pathological conditions that have been attributed to an accumulation of misfolded proteins in the ER have previously been correlated with a disruption in $Ca^{2+}$ homeostasis [13, 58]. Our experiments investigated this relationship at much higher sensitivity. We utilized the more physiological relevant expression of a normally secreted single protein, CPY-wt, along with its folding mutant, $CPY_{G255R}$, which was known to be retained in the ER. We determined that expression of the folding mutant did not induce a detectable change in the level of ER $Ca^{2+}$. It is possible that our $Ca^{2+}$ indicator probe was not sufficiently sensitive. However, expression of the $CPY_{G255R}$ folding mutant also failed to initiate a significant UPR, consistent with the absence of a detectable $Ca^{2+}$ leak. Consequently, we interpreted these results as evidence that the accumulation of a single misfolded protein, at least under our conditions, was not sufficient to induce either a $Ca^{2+}$ leak or an ER stress response. However, both were observed when we generally disrupted protein folding in *Xenopus* oocytes with Tn treatment. It had previously been reported that Tn induced $Ca^{2+}$ mobilization from the ER in SV40-transformed human fibroblasts [59], CHO cells [60] and HeLa cells [41]. Work from our group also reported a sustained increase in cytosolic $Ca^{2+}$ that occurred within minutes of Tn treatment in *Xenopus* oocytes [47]. We extended these findings here by demonstrating that Tn treatment of *Xenopus* oocytes effectively induces the UPR. A simple explanation of the disparity between single and general protein misfolding is that *Xenopus* oocytes are not sensitive to ER stress caused by a single misfolded protein due to their inherent capacity to express large quantities of proteins. Throughout the text, we have equated the luminal ER accumulation of CPY-wt and its mutant ($CPY_{G255R}$) to misfolded proteins, and note here that this accumulation can be attributed to defects in multiple processes including protein synthesis, folding and secretion and ER associated degradation system (ERAD) [61–63].

Under resting conditions, the ER intraluminal free calcium concentration reflects a balance between active uptake by $Ca^{2+}$-ATPases and passive efflux via leak channels. Several research groups have proposed that a basal $Ca^{2+}$ leak occurs via the translocon [24–27]. This is an aqueous pore that completely spans the ER lipid bilayer [29] through which newly synthesized secretory proteins are translocated [64]. The heteromeric Sec61 complex forms the core of this pore, which is blocked by the ribosome on the cytosolic side and by BiP on the luminal side [65]. Recently, Zimmermann's group [48] reported that under protein misfolding accumulation, BiP is involved in gating of the translocon channel subunit Sec61, allowing $Ca^{2+}$ leak from the ER. They also demonstrated that calmodulin limited this leak, in a $Ca^{2+}$-dependent manner by binding to a cytosolic Sec61 motif [66]. Moreover, a point mutation in the Sec61 channel (Sec61alpha1Y344H) could not be gated by BiP. Previous work indicated that this mutation disrupted ER homeostasis leading to Beta-cells apoptosis in a diabetes mouse model [67].

Consistent with these findings, our data shows that $Ca^{2+}$ leak can be a cause and a consequence of the UPR. This leak probably occurs due to a dissociation of BiP from the translocon upon association of this chaperone to misfolded proteins under conditions of ER stress therefore leaving the translocon "unplugged" from the luminal side. The loss of BiP from the translocon can greatly enhance the magnitude of the UPR regardless of the stress inducer by mediating phosphorylation of elF2α through the $Ca^{2+}$ signal initiated by the leak.

In summary, our data show that a stress-induced $Ca^{2+}$ leak, likely via the translocon channel, is a crucial signal required for activation of the UPR. We note that emetine treatment did not completely block the $Ca^{2+}$ leak under ER stress nor did it completely inhibit phosphorylation of elF2α, or BiP expression. Thus, we cannot rule out the possibility that a different protein, other than Sec61, could be also responsible for leaking $Ca^{2+}$ from ER stores during the early phase of ER stress, such as: presenilins [53], Bcl2 [39, 68], ST1 [69], $IP_3Rs$ [70], RyRs [71]. Irrespective of the identity of the $Ca^{2+}$ link channel, our data demonstrate a critical link between stressinduced $Ca^{2+}$ release and the initiation of the UPR.

## Supplementary Material

Refer to Web version on PubMed Central for supplementary material.

## Acknowledgments

This work was funded in part by the National Institutes of Health (NIH) grants [R01 AG029461] and [P01 AG19316].

We thank Dr. Lee McAlister-Henn (University of Texas Health Science Center at San Antonio) for providing the DNA library of *Saccharomyces cerevisiae* and Dr. Roger Tsien (University of California / Howard Hughes Medical Institute) for providing the mStrawberry (mStr), mCyan fluorescent protein (mCFP) and D1ER constructs.

## References

1. Alberts, BJ.; Lewis, A.; Raff, J.; Robberts, M.; Walter, P, K. Garland Science. New York, NY: 2002. Molecular Biology of the Cell.
2. Hammond C, Helenius A. Quality control in the secretory pathway. Curr Opin Cell Biol. 1995; 7:523–529. [PubMed: 7495572]
3. Berridge MJ. The endoplasmic reticulum: a multifunctional signaling organelle. Cell Calcium. 2002; 32:235–249. [PubMed: 12543086]
4. Li Y, Camacho P. Ca2+-dependent redox modulation of SERCA 2b by ERp57. J Cell Biol. 2004; 164:35–46. [PubMed: 14699087]
5. Meldolesi J, Pozzan T. The endoplasmic reticulum Ca2+ store: a view from the lumen. Trends Biochem Sci. 1998; 23:10–14. [PubMed: 9478128]
6. Roderick HL, Lechleiter JD, Camacho P. Cytosolic phosphorylation of calnexin controls intracellular Ca(2+) oscillations via an interaction with SERCA2b. Cell. Biol. J. 2000; 149:1235–1248.
7. Burdakov D, Petersen OH, Verkhratsky A. Intraluminal calcium as a primary regulator of endoplasmic reticulum function. Cell Calcium. 2005; 38:303–310. [PubMed: 16076486]
8. Schroder M, Kaufman RJ. ER stress and the unfolded protein response. Mutat Res. 2005; 569:29–63. [PubMed: 15603751]
9. Harding HP, Zhang Y, Ron D. Protein translation and folding are coupled by an endoplasmic-reticulum-resident kinase. Nature. 1999; 397:271–274. [PubMed: 9930704]
10. Scorrano L, Oakes SA, Opferman JT, Cheng EH, Sorcinelli MD, Pozzan T, Korsmeyer SJ. BAX and BAK regulation of endoplasmic reticulum Ca2+: a control point for apoptosis. Science. 2003; 300:135–139. [PubMed: 12624178]

11. Leissring MA, Paul BA, Parker I, Cotman CW, LaFerla FM. Alzheimer's presenilin-1 mutation potentiates inositol 1,4,5-trisphosphate-mediated calcium signaling in Xenopus oocytes. J Neurochem. 1999; 72:1061–1068. [PubMed: 10037477]
12. Arduino DM, Esteves AR, Cardoso SM, Oliveira CR. Endoplasmic reticulum and mitochondria interplay mediates apoptotic cell death: relevance to Parkinson's disease. Neurochem. Int. 2009; 55:341–348. [PubMed: 19375464]
13. Hetz C, Russelakis-Carneiro M, Maundrell K, Castilla J, Soto C. Caspase-12 and endoplasmic reticulum stress mediate neurotoxicity of pathological prion protein. Embo J. 2003; 22:5435–5445. [PubMed: 14532116]
14. Haughey NJ, Holden CP, Nath A, Geiger JD. Involvement of inositol 1,4,5-trisphosphateregulated stores of intracellular calcium in calcium dysregulation and neuron cell death caused by HIV-1 protein tat. J Neurochem. 1999; 73:1363–1374. [PubMed: 10501179]
15. Cnop M, Welsh N, Jonas JC, Jorns A, Lenzen S, Eizirik DL. Mechanisms of pancreatic beta-cell death in type 1 and type 2 diabetes: many differences few similarities. Diabetes. 2005; 54(Suppl 2):S97–S107. [PubMed: 16306347]
16. Lindholm D, Wootz H, Korhonen L. ER stress and neurodegenerative diseases. Cell Death Differ. 2006; 13:385–392. [PubMed: 16397584]
17. Yoshida H. ER stress and diseases. FEBS J. 2007; 274:630–658. [PubMed: 17288551]
18. Zhao L, Ackerman SL. Endoplasmic reticulum stress in health and disease. Curr Opin Cell Biol. 2006; 18:444–452. [PubMed: 16781856]
19. Nakagawa T, Zhu H, Morishima N, Li E, Xu J, Yankner BA, Yuan J. Caspase-12 mediates endoplasmic-reticulum-specific apoptosis and cytotoxicity by amyloid-beta. Nature. 2000; 403:98–103. [PubMed: 10638761]
20. Wong WL, Brostrom MA, Kuznetsov G, Gmitter-Yellen D, Brostrom CO. Inhibition of protein synthesis and early protein processing by thapsigargin in cultured cells. Biochem J. 1993; 289(Pt 1):71–79. [PubMed: 8424774]
21. Lytton J, Westlin M, Hanley MR. Thapsigargin inhibits the sarcoplasmic or endoplasmic reticulum Ca-ATPase family of calcium pumps. J Biol Chem. 1991; 266:17067–17071. [PubMed: 1832668]
22. Lytton J, Westlin M, Burk SE, Shull GE, MacLennan DH. Functional comparisons between isoforms of the sarcoplasmic or endoplasmic reticulum family of calcium pumps. J Biol Chem. 1992; 267:14483–14489. [PubMed: 1385815]
23. Hofer AM, Curci S, Machen TE, Schulz I. ATP regulates calcium leak from agonist-sensitive internal calcium stores. Faseb J. 1996; 10:302–308. [PubMed: 8641563]
24. Ong HL, Liu X, Sharma A, Hegde RS, Ambudkar IS. Intracellular Ca(2+) release via the ER translocon activates store-operated calcium entry. Pflugers Arch. 2007; 453:797–808. [PubMed: 17171366]
25. Van Coppenolle F, Vanden Abeele F, Slomianny C, Flourakis M, Hesketh J, Dewailly E, Prevarskaya N. Ribosome-translocon complex mediates calcium leakage from endoplasmic reticulum stores. J Cell Sci. 2004; 117:4135–4142. [PubMed: 15280427]
26. Flourakis M, Van Coppenolle F, Lehen'kyi V, Beck B, Skryma R, Prevarskaya N. Passive calcium leak via translocon is a first step for iPLA2-pathway regulated store operated channels activation. FASEB J. 2006; 20:1215–1217. [PubMed: 16611832]
27. Giunti R, Gamberucci A, Fulceri R, Banhegyi G, Benedetti A. Both translocon and a cation channel are involved in the passive Ca2+ leak from the endoplasmic reticulum: a mechanistic study on rat liver microsomes. Arch Biochem Biophys. 2007; 462:115–121. [PubMed: 17481572]
28. Lomax RB, Camello C, Van Coppenolle F, Petersen OH, Tepikin AV. Basal and physiological Ca(2+) leak from the endoplasmic reticulum of pancreatic acinar cells. Second messenger-activated channels and translocons. J Biol Chem. 2002; 277:26479–26485. [PubMed: 11994289]
29. Crowley KS, Liao S, Worrell VE, Reinhart GD, Johnson AE. Secretory proteins move through the endoplasmic reticulum membrane via an aqueous, gated pore. Cell. 1994; 78:461–471. [PubMed: 8062388]
30. Swanton E, Bulleid NJ. Protein folding and translocation across the endoplasmic reticulum membrane. Mol Membr Biol. 2003; 20:99–104. [PubMed: 12851067]

31. Erdmann F, Schauble N, Lang S, Jung M, Honigmann A, Ahmad M, Dudek J, Benedix J, Harsman A, Kopp A, Helms V, Cavalie A, Wagner R, Zimmermann R. Interaction of calmodulin with Sec61alpha limits Ca2+ leakage from the endoplasmic reticulum. EMBO J. 2011; 30:17–31. [PubMed: 21102557]
32. Schauble N, Lang S, Jung M, Cappel S, Schorr S, Ulucan O, Linxweiler J, Dudek J, Blum R, Helms V, Paton AW, Paton JC, Cavalie A, Zimmermann R. BiP-mediated closing of the Sec61 channel limits Ca2+ leakage from the ER. EMBO J. 2012; 31:3282–3296. [PubMed: 22796945]
33. Yoshida I, Monji A, Tashiro K, Nakamura K, Inoue R, Kanba S. Depletion of intracellular Ca2+ store itself may be a major factor in thapsigargin-induced ER stress and apoptosis in PC12 cells. Neurochem Int. 2006; 48:696–702. [PubMed: 16481070]
34. Mancini R, Aebi M, Helenius A. Multiple endoplasmic reticulum-associated pathways degrade mutant yeast carboxypeptidase Y in mammalian cells. J Biol Chem. 2003; 278:46895–46905. [PubMed: 12954632]
35. Finger A, Knop M, Wolf DH. Analysis of two mutated vacuolar proteins reveals a degradation pathway in the endoplasmic reticulum or a related compartment of yeast. Eur J Biochem. 1993; 218:565–574. [PubMed: 8269947]
36. Camacho P, Lechleiter JD. Calreticulin inhibits repetitive intracellular Ca2+ waves. Cell. 1995; 82:765–771. [PubMed: 7671304]
37. Roderick HL, Lechleiter JD, Camacho P. Cytosolic phosphorylation of calnexin controls intracellular Ca(2+) oscillations via an interaction with SERCA2b. J Cell Biol. 2000; 149:1235–1248. [PubMed: 10851021]
38. Prouty AM, Wu J, Lin DT, Camacho P, Lechleiter JD. Multiphoton laser scanning microscopy as a tool for Xenopus oocyte research. Methods Mol Biol. 2006; 322:87–101. [PubMed: 16739718]
39. Palmer AE, Jin C, Reed JC, Tsien RY. Bcl-2-mediated alterations in endoplasmic reticulum Ca2+ analyzed with an improved genetically encoded fluorescent sensor. Proc Natl Acad Sci U S A. 2004; 101:17404–17409. [PubMed: 15585581]
40. Lodish HF, Kong N, Wikstrom L. Calcium is required for folding of newly made subunits of the asialoglycoprotein receptor within the endoplasmic reticulum. J Biol Chem. 1992; 267:12753–12760. [PubMed: 1618778]
41. Deniaud A, Sharaf el dein O, Maillier E, Poncet D, Kroemer G, Lemaire C, Brenner C. Endoplasmic reticulum stress induces calcium-dependent permeability transition, mitochondrial outer membrane permeabilization and apoptosis. Oncogene. 2008; 27:285–299. [PubMed: 17700538]
42. Wang Q, Zhang H, Zhao B, Fei H. IL-1beta caused pancreatic beta-cells apoptosis is mediated in part by endoplasmic reticulum stress via the induction of endoplasmic reticulum Ca2+ release through the c-Jun N-terminal kinase pathway. Mol Cell Biochem. 2009; 324:183–190. [PubMed: 19109696]
43. So J, Warsh JJ, Li PP. Impaired endoplasmic reticulum stress response in B-lymphoblasts from patients with bipolar-I disorder. Biol Psychiatry. 2007; 62:141–147. [PubMed: 17217928]
44. Bertolotti A, Zhang Y, Hendershot LM, Harding HP, Ron D. Dynamic interaction of BiP and ER stress transducers in the unfolded-protein response. Nat. Cell. Biol. 2000; 2:326–332. [PubMed: 10854322]
45. Liu CY, Schroder M, Kaufman RJ. Ligand-independent dimerization activates the stress response kinases IRE1 and PERK in the lumen of the endoplasmic reticulum. J Biol Chem. 2000; 275:24881–24885. [PubMed: 10835430]
46. Falcke M, Li Y, Lechleiter JD, Camacho P. Modeling the dependence of the period of intracellular Ca2+ waves on SERCA expression. Biophys J. 2003; 85:1474–1481. [PubMed: 12944265]
47. Bollo M, Paredes RM, Holstein D, Zheleznova N, Camacho P, Lechleiter JD. Calcineurin interacts with PERK and dephosphorylates calnexin to relieve ER stress in mammals and frogs. PloS one. 2010; 5:e11925. [PubMed: 20700529]
48. Schauble N, Lang S, Jung M, Cappel S, Schorr S, Ulucan O, Linxweiler J, Dudek J, Blum R, Helms V, Paton AW, Paton JC, Cavalie A, Zimmermann R. BiP-mediated closing of the Sec61 channel limits Ca(2+) leakage from the ER. The EMBO journal. 2012; 31:3282–3296. [PubMed: 22796945]

49. Lin JH, Li H, Yasumura D, Cohen HR, Zhang C, Panning B, Shokat KM, Lavail MM, Walter P. IRE1 signaling affects cell fate during the unfolded protein response. Science. 2007; 318:944–949. [PubMed: 17991856]
50. Cox DJ, Strudwick N, Ali AA, Paton AW, Paton JC, Schroder M. Measuring signaling by the unfolded protein response. Methods Enzymol. 2011; 491:261–292. [PubMed: 21329805]
51. Marciniak SJ, Yun CY, Oyadomari S, Novoa I, Zhang Y, Jungreis R, Nagata K, Harding HP, Ron D. CHOP induces death by promoting protein synthesis and oxidation in the stressed endoplasmic reticulum. Genes Dev. 2004; 18:3066–3077. [PubMed: 15601821]
52. Koumenis C, Naczki C, Koritzinsky M, Rastani S, Diehl A, Sonenberg N, Koromilas A, Wouters BG. Regulation of protein synthesis by hypoxia via activation of the endoplasmic reticulum kinase PERK and phosphorylation of the translation initiation factor eIF2alpha. Mol Cell Biol. 2002; 22:7405–7416. [PubMed: 12370288]
53. Tu H, Nelson O, Bezprozvanny A, Wang Z, Lee SF, Hao YH, Serneels L, De Strooper B, Yu G, Bezprozvanny I. Presenilins form ER Ca2+ leak channels, a function disrupted by familial Alzheimer's disease-linked mutations. Cell. 2006; 126:981–993. [PubMed: 16959576]
54. Smith IF, Boyle JP, Kang P, Rome S, Pearson HA, Peers C. Hypoxic regulation of Ca2+ signaling in cultured rat astrocytes. Glia. 2005; 49:153–157. [PubMed: 15390111]
55. Park SW, Zhou Y, Lee J, Ozcan U. Sarco(endo)plasmic reticulum Ca2+-ATPase 2b is a major regulator of endoplasmic reticulum stress and glucose homeostasis in obesity. Proc Natl Acad Sci U S A. 2010; 107:19320–19325. [PubMed: 20974941]
56. Ozcan U, Cao Q, Yilmaz E, Lee AH, Iwakoshi NN, Ozdelen E, Tuncman G, Gorgun C, Glimcher LH, Hotamisligil GS. Endoplasmic reticulum stress links obesity, insulin action, and type 2 diabetes. Science. 2004; 306:457–461. [PubMed: 15486293]
57. Wojda U, Salinska E, Kuznicki J. Calcium ions in neuronal degeneration. IUBMB Life. 2008; 60:575–590. [PubMed: 18478527]
58. Benali-Furet NL, Chami M, Houel L, De Giorgi F, Vernejoul F, Lagorce D, Buscail L, Bartenschlager R, Ichas F, Rizzuto R, Paterlini-Brechot P. Hepatitis C virus core triggers apoptosis in liver cells by inducing ER stress and ER calcium depletion. Oncogene. 2005; 24:4921–4933. [PubMed: 15897896]
59. Carlberg M, Dricu A, Blegen H, Kass GE, Orrenius S, Larsson O. Short exposures to tunicamycin induce apoptosis in SV40-transformed but not in normal human fibroblasts. Carcinogenesis. 1996; 17:2589–2596. [PubMed: 9006093]
60. Hayashi T, Su TP. Sigma-1 receptor chaperones at the ER-mitochondrion interface regulate Ca(2+) signaling and cell survival. Cell. 2007; 131:596–610. [PubMed: 17981125]
61. Buchberger A, Bukau B, Sommer T. Protein quality control in the cytosol and the endoplasmic reticulum: brothers in arms. Molecular cell. 2010; 40:238–252. [PubMed: 20965419]
62. Kawaguchi S, Hsu CL, Ng DT. Interplay of substrate retention and export signals in endoplasmic reticulum quality control. PloS one. 2010; 5:e15532. [PubMed: 21151492]
63. Hebert DN, Molinari M. In and out of the ER: protein folding, quality control, degradation, and related human diseases. Physiological reviews. 2007; 87:1377–1408. [PubMed: 17928587]
64. Hanein D, Matlack KE, Jungnickel B, Plath K, Kalies KU, Miller KR, Rapoport TA, Akey CW. Oligomeric rings of the Sec61p complex induced by ligands required for protein translocation. Cell. 1996; 87:721–732. [PubMed: 8929540]
65. Hamman BD, Hendershot LM, Johnson AE. BiP maintains the permeability barrier of the ER membrane by sealing the lumenal end of the translocon pore before and early in translocation. Cell. 1998; 92:747–758. [PubMed: 9529251]
66. Lang S, Erdmann F, Jung M, Wagner R, Cavalie A, Zimmermann R. Sec61 complexes form ubiquitous ER Ca2+ leak channels. Channels (Austin). 2011; 5:228–235. [PubMed: 21406962]
67. Lloyd DJ, Wheeler MC, Gekakis N. A point mutation in Sec61alpha1 leads to diabetes and hepatosteatosis in mice. Diabetes. 2010; 59:460–470. [PubMed: 19934005]
68. Pinton P, Ferrari D, Magalhaes P, Schulze-Osthoff K, Di Virgilio F, Pozzan T, Rizzuto R. Reduced loading of intracellular Ca(2+) stores and downregulation of capacitative Ca(2+) influx in Bcl-2-overexpressing cells. J Cell Biol. 2000; 148:857–862. [PubMed: 10704437]

69. Chami M, Oules B, Szabadkai G, Tacine R, Rizzuto R, Paterlini-Brechot P. Role of SERCA1 truncated isoform in the proapoptotic calcium transfer from ER to mitochondria during ER stress. Mol Cell. 2008; 32:641–651. [PubMed: 19061639]

70. Cheung KH, Shineman D, Muller M, Cardenas C, Mei L, Yang J, Tomita T, Iwatsubo T, Lee VM, Foskett JK. Mechanism of Ca2+ disruption in Alzheimer's disease by presenilin regulation of InsP3 receptor channel gating. Neuron. 2008; 58:871–883. [PubMed: 18579078]

71. Stutzmann GE, Smith I, Caccamo A, Oddo S, Laferla FM, Parker I. Enhanced ryanodine receptor recruitment contributes to Ca2+ disruptions in young, adult, and aged Alzheimer's disease mice. J Neurosci. 2006; 26:5180–5189. [PubMed: 16687509]

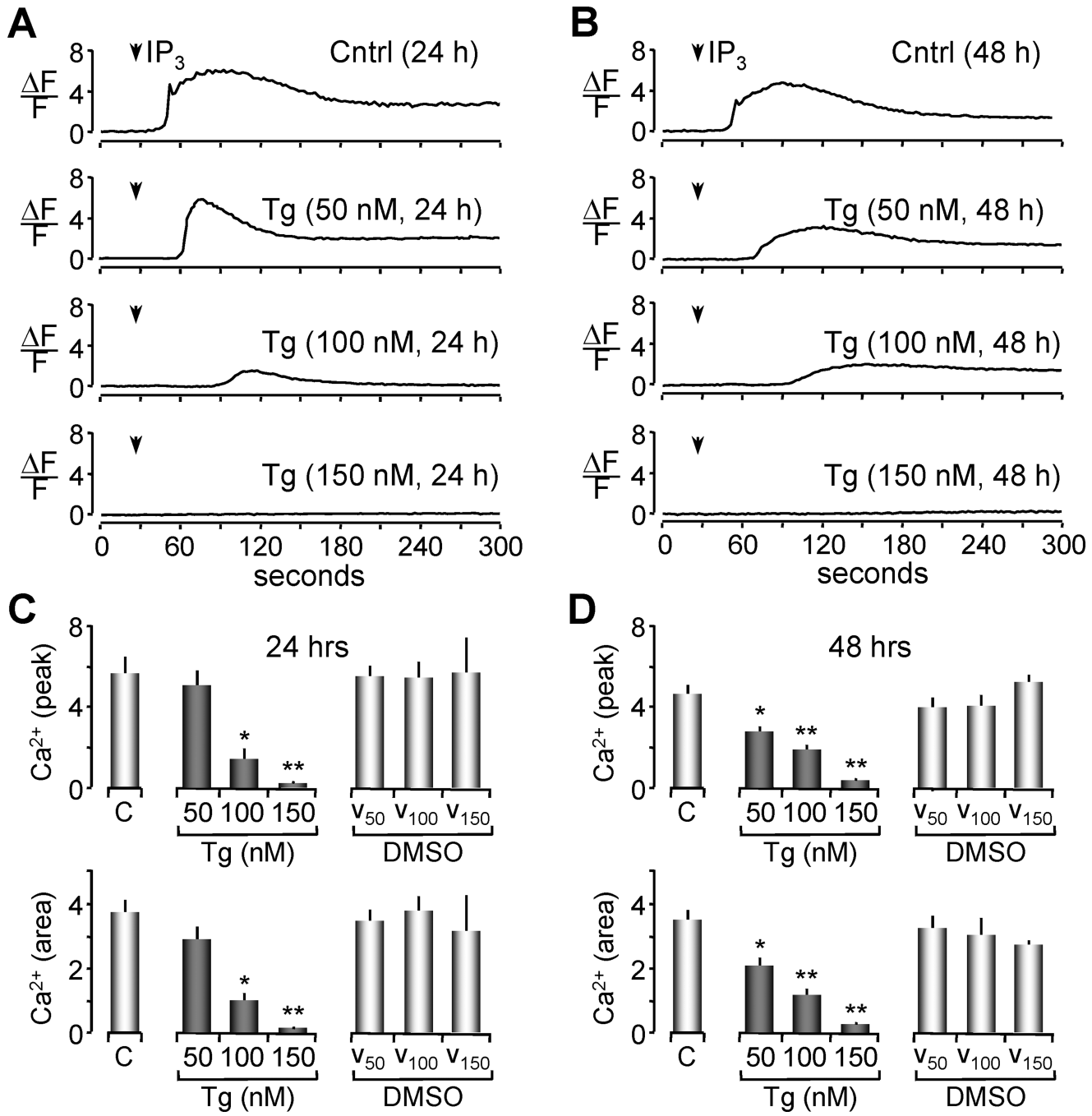


**Figure 1. Depletion of luminal $Ca^{2+}$ by thapsigargin is reflected as a decrease in $Ca^{2+}$ release**

(A-B) Measurement of ER $Ca^{2+}$ content by confocal imaging of *Xenopus* oocytes loaded with fluo-4. Representative traces of fluorescence measurements of $IP_3$ induced $Ca^{2+}$ release are shown. 300 nM $IP_3$ was injected 40 seconds after the beginning of the recording for all groups as indicated by the arrow. Traces represent changes in fluorescence from resting levels as a function of time (ΔF/F) for 24 hrs treatment (A) and 48 hrs Tg treatment (B). The ΔF/F measure of $IP_3$ induced releasable $Ca^{2+}$ was obtained by selecting a 5×5 pixel area from subsequent images obtained during imaging of individual oocytes.

(C-D) Histograms of the $Ca^{2+}$ release after $IP_3$ injection shown in A in terms of the peak of amplitude (top) or in terms of the area under the curve (bottom) are represented as the means

± SEM of untreated groups (control, C), Tg treated and DMSO (vehicle control) at 24 (C) or 48 (D) hrs of treatment. Values are from n = 3–16 oocytes per group from two independent experiments. Asterisks indicate statistical significance (*p<0.05, **p<0.01, ANOVA).

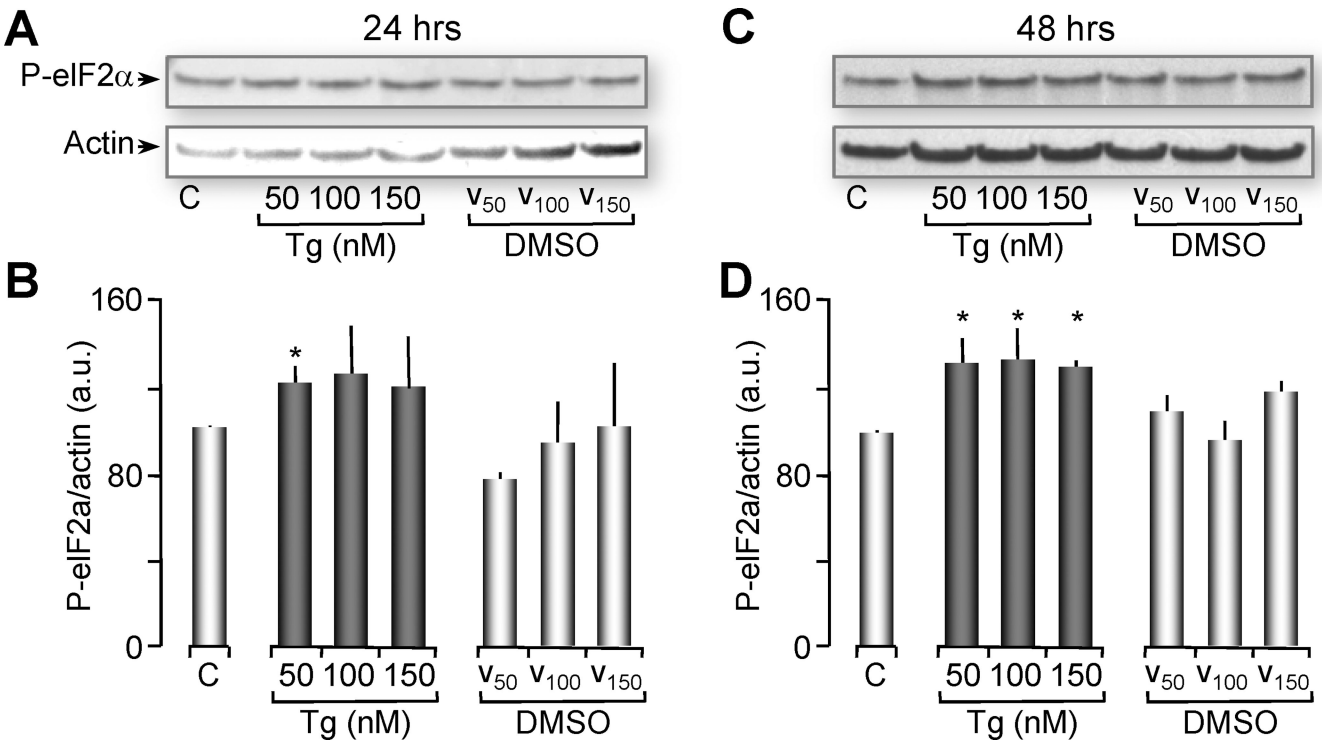


**Figure 2. Thapsigargin treatment induces phosphorylation of eIF2α (ER Stress marker)**

(A) Western blot showing phosphorylation levels of eIF2α (ER stress marker) from oocytes treated with Tg or vehicle (DMSO) for 24 hrs. Two oocyte equivalents were loaded per lane and proteins were resolved through 12% SDS-PAGE. Actin western blot is shown as loading control. These gels represent 4 independent western blots with n=20 oocytes per group per experiment.

(B) Histograms of the ratio of P-eIF2α normalized with actin (shown in A and C) are represented as the mean ± SEM. Asterisks indicate statistical significance (*p<0.05, ANOVA).

(C) Similarly as in A, western blot of P-eIF2α from oocytes treated with Tg or vehicle (DMSO) for 48 hrs. These gels represent 4 independent western blots, n=20 oocytes per group.

(D) Histograms of the ratio P-eIF2α normalized with actin are represented as the mean ± SEM. Asterisks indicate statistical significance (*p<0.05, ANOVA).

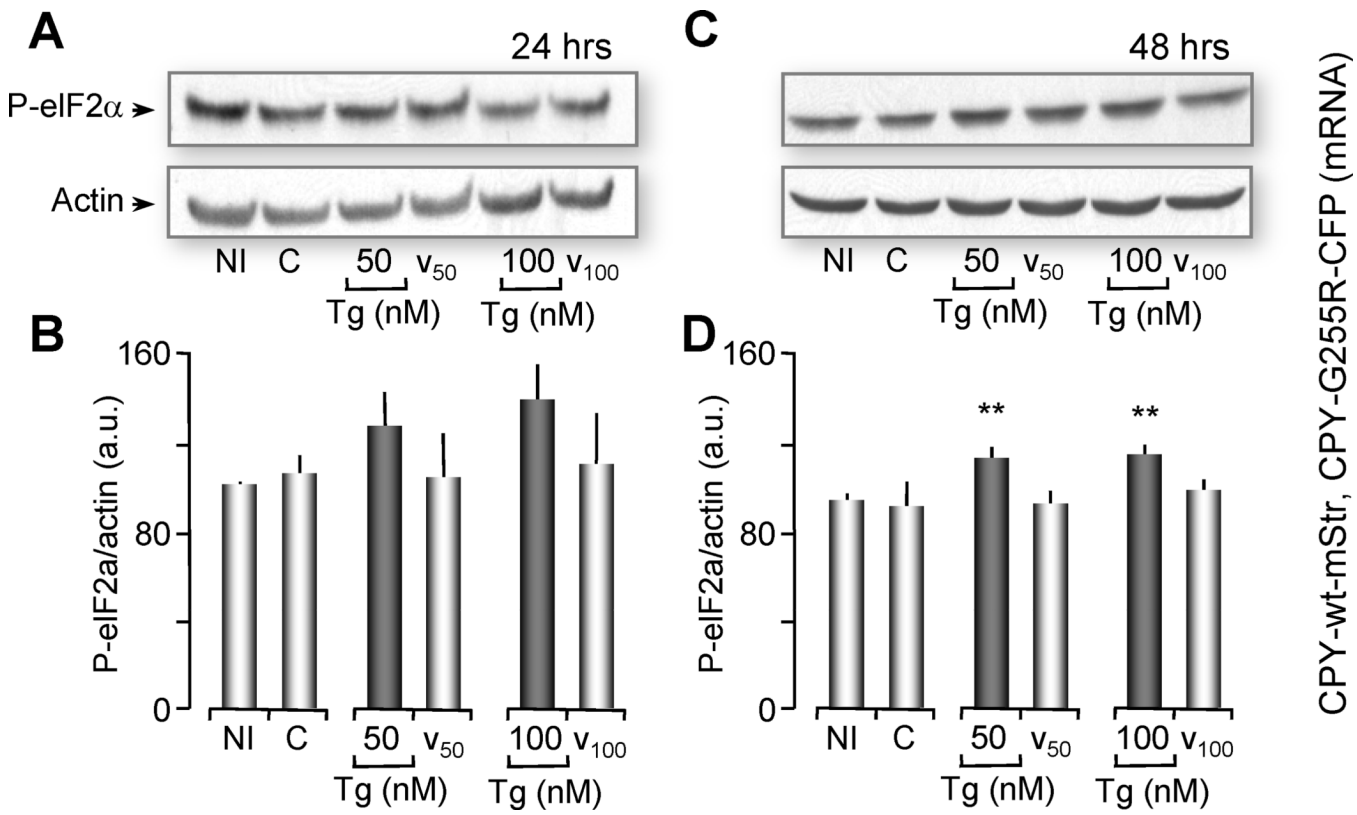


**Figure 3. 48 Hours of Partial $Ca^{2+}$ Depletion, induces ER Stress in Oocytes co-expressing CPY-wt and CPY-mutant**

(A, C) Western blot of P-eIF2α (ER stress marker) from oocytes injected with a combination of mRNA of CPY-wt-mStr and mutant $CPY_{G255R}$-CFP or non-injected (NI) as indicated. Oocytes were untreated (C) or treated with 50 or 100 nM Tg or vehicle for 24 hrs (A) or 48 hrs (C). Two oocyte equivalents were loaded per lane and proteins were resolved through 12% SDS-PAGE. Actin western blot was used as loading control. These gels represent 3 independent western blots, n=20 oocytes per group. (B, D) Histograms of the ratio P-eIF2α normalized with actin for 24 hrs (B) or 48 hrs (D) are represented as the means ± SEM. Asterisks indicate statistical significance (**p<0.01 ANOVA). Note that ER stress is induced after 48 hours of partial $Ca^{2+}$ depletion but not after 24 hours.

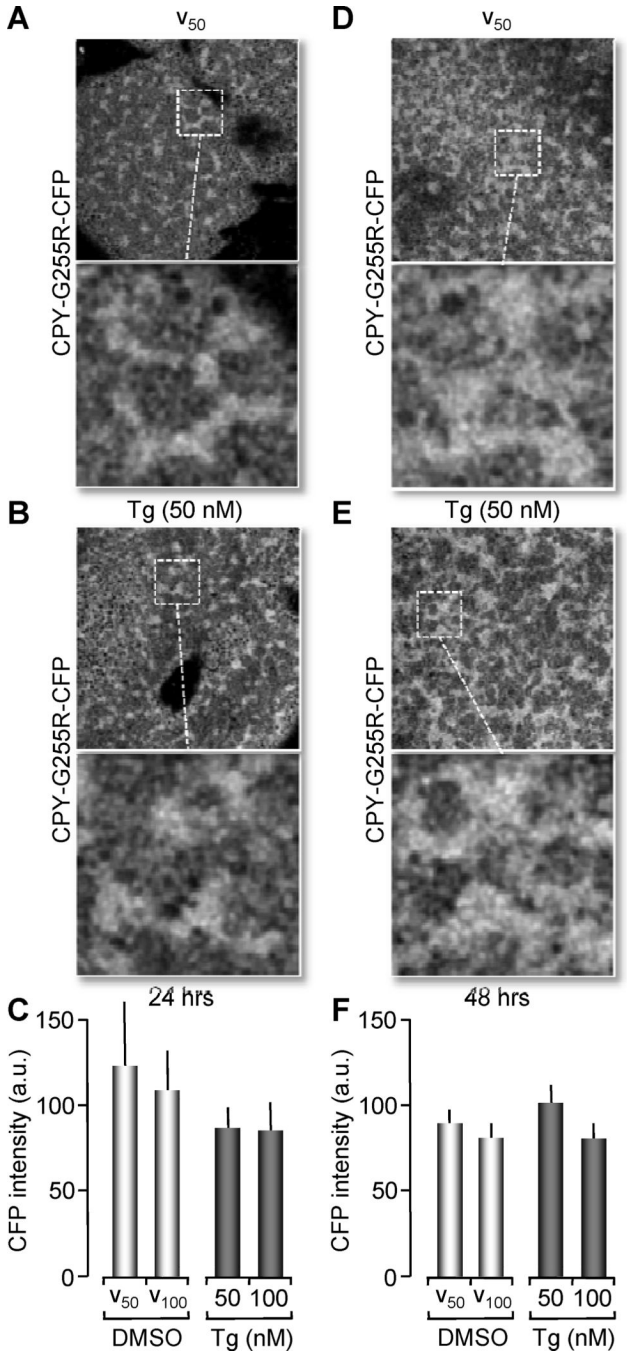


**Figure 4. $CPY_{G255R}$-CFP luminal retention is maintained in untreated or Tg treated oocytes**

(A, B, D and E) Confocal images of *Xenopus* oocytes co-expressing $CPY_{G255R}$-CFP and CPY-wt-mStr. Images collected using CFP channel (458nm, Argon laser) for excitation to detect only $CPY_{G255R}$-CFP fluorescence. 24 hrs after mRNA injection, oocytes were treated with 50 nM Tg (shown here in B), 100 nM Tg (not shown) or vehicle for 24 hrs (A). Also shown images of 48 hrs of treatment with vehicle (D) or 50 nM Tg (E). Confocal images were obtained with a 63× objective NA 1.4 oil immersion objective. A magnified image from a region in the field is shown to depict ER like structures. (C, F) Histograms representing fluorescence intensity of ER like structures from CFP emission after 24 hrs treatment (C) or 48 hrs (F) was comparable between Tg treated and vehicle treated oocytes

(no statistical significance). Data were plotted as the ratio of fluorescence obtained for Tg normalized with vehicle and vehicle was normalized with fluorescence of untreated oocytes. Histograms of the ratio values are represented as the means ± SEM. Data pooled from 5 independent experiments, n=8–10 oocytes per group per experiment.

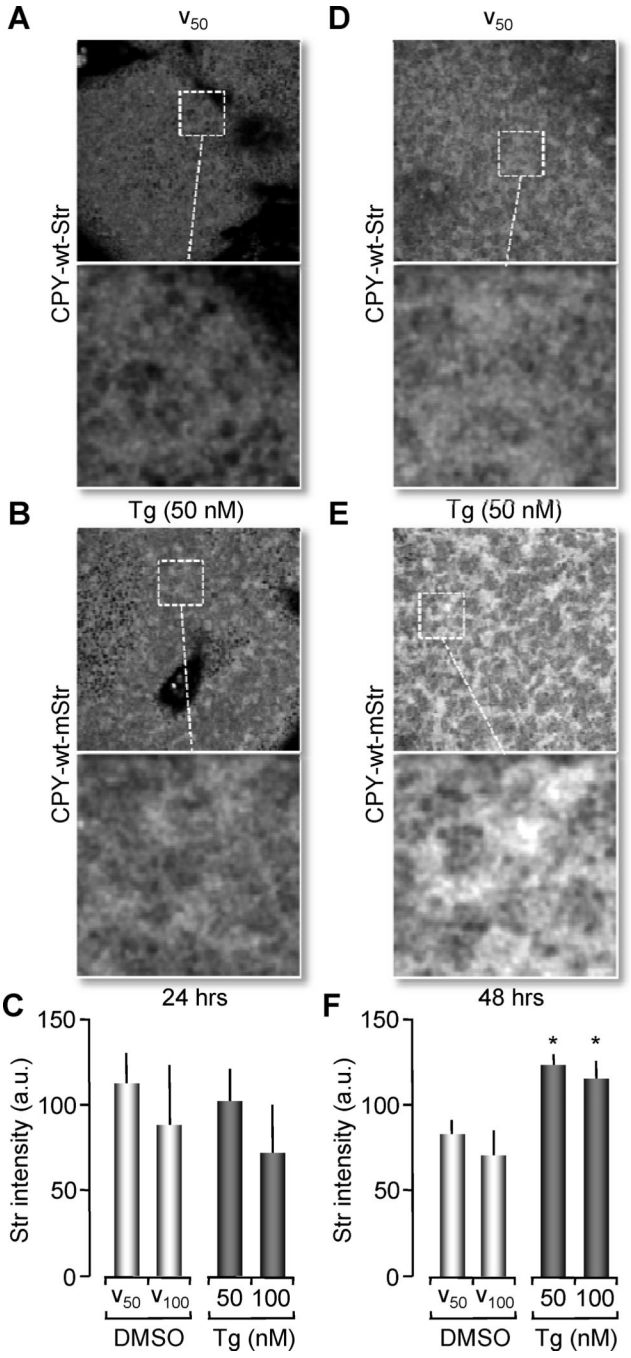


**Figure 5. Wild type CPY-Str is only retained in the ER by partial $Ca^{2+}$ depletion (Tg treatment)**

(A, B, D and E) Confocal images of *Xenopus* oocytes co-expressing $CPY_{G255R}$-CFP and CPY-wt-Str. Images collected using STR channel (543nm, Helium-Neon Laser) for excitation to detect only CPY-wt- Str fluorescence. 24 hrs after mRNA injection, oocytes were treated with 50 nM Tg (shown here in B), 100 nM Tg (not shown) or vehicle for 24 hrs (A). Also shown images of 48 hrs of treatment with vehicle (D) or 50 nM Tg (E). Confocal images were obtained with a 63× objective NA 1.4 oil immersion objective. A magnified image from a region in the field is shown to depict ER like structures. (C, F) Histograms representing fluorescence intensity of ER like structures from Str emission after 24 hrs treatment (C) or 48 hrs (F) were higher at 48 hrs Tg treatment with statistical significance

(*p<0.05, ANOVA). Histograms of the ratio values are represented as the means ± SEM. Data pooled from 5 independent experiments, n=8–10 oocytes per group per experiment.

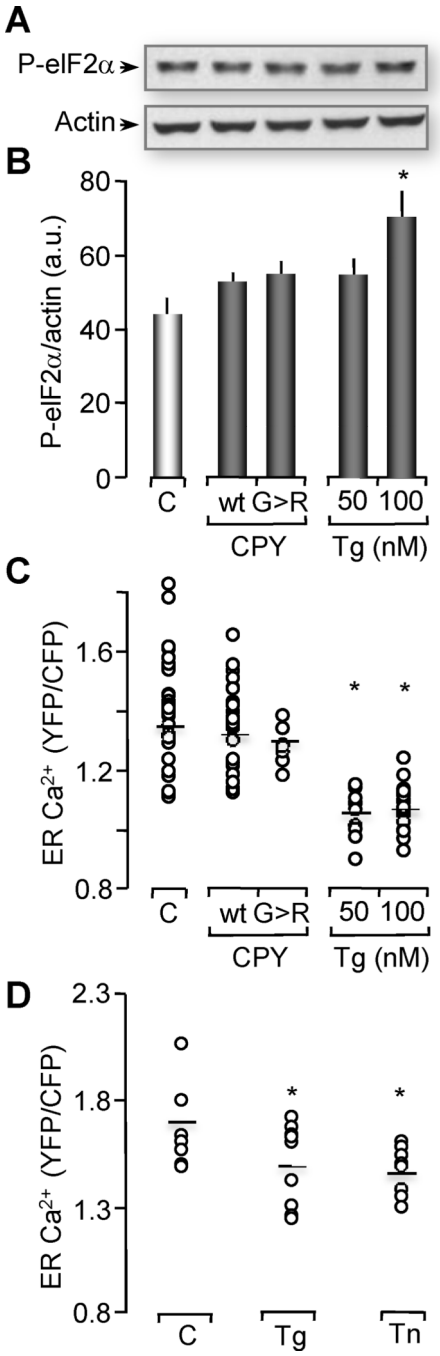


**Figure 6. *Xenopus* oocytes injected with $CPY_{G255R}$ mRNA do not exhibit changes in ER $Ca^{2+}$ or stress**

(A) Western blot of phosphorylation levels of eIF2α from untreated oocytes (C) over-expressing D1ER as $Ca^{2+}$ indicator, D1ER expressing oocytes treated with 50 nM or 100 nM Tg for 24 hrs or oocytes coexpressing D1ER with CPY-wt (wt) or co-expressing D1ER with mutant $CPY_{G255R}$ (G>R). Two oocyte equivalents were loaded per lane and proteins were resolved through 12% SDS-PAGE. Actin western blot is shown as loading control. Gels represent 4 independent western blots with 15–20 oocytes per group.

(B) Histograms of the ratio of P-eIF2α normalized with actin are represented as the means ± SEM. Asterisks indicate statistical significance (*$p<0.05$, ANOVA). Notice that ER stress was only induced with 100 nM Tg treatment, but no with $CPY_{G255R}$.
(C) ER $Ca^{2+}$ levels measured by the emission ratio of YFP/CFP in D1ER were plotted as the mean values of individual oocytes. Tg treatment in this experiment was performed for 24 hrs. Data distribution was obtained from 2–6 independent experiments with n= 8–28 oocytes analyzed per group.
Asterisks indicate statistical significance (ANOVA, *$p<0.05$). Notice that Tg-induced $Ca^{2+}$depletion of the ER was successfully observed with the D1ER indicator. However, no changes in ER $Ca^{2+}$ levels were observed with $CPY_{G255R}$ (G>R), or CPY-wt (wt) when compared to control oocytes.
(D) ER $Ca^{2+}$ levels were measured and plotted as is indicated in (C). 50 nM Tg treatment was performed for 24 hrs, Tn treatment was performed for 2 hrs. Data distribution was obtained from n= 10 oocytes analyzed per group, (ANOVA, *$p<0.05$). Notice that ER $Ca^{2+}$ levels after treatment with Tn for 2 hrs is comparable with 50 nM Tg treatment for 24 hrs.

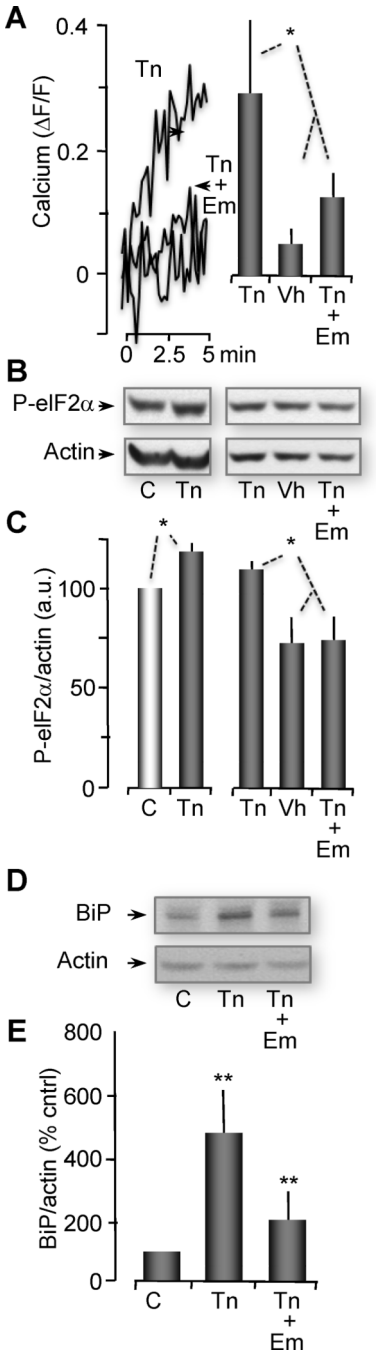


**Figure 7. Emetine, a translocon inhibitor, blocks ER $Ca^{2+}$ leak and ER stress induced by tunicamycin**

(A) (Left) Representative traces of cytosolic $Ca^{2+}$ change in terms of ΔF/F fluorescence intensity. Data were obtained from oocytes incubated for 2 hrs with 2.5 μg/ml tunicamycin alone (Tn), 0.05% vehicle (Vh) or tunicamycin plus emetine (Tn + Em). For emetine treated oocytes, the last 30 min of incubation with Tn or vehicle were done in the presence of 1 μM emetine. To observe cytosolic $Ca^{2+}$ changes, all groups were injected with 50 μM fluo-4 30 min before confocal imaging (performed for 5 min). (Right) Histograms represent the change in cytosolic $Ca^{2+}$ levels (in terms of fluo-4, ΔF/F) between time 0 (rest) to the highest peak after 5 min of imaging (obtained from traces shown on left panel). Histograms

represented as the mean ± SEM. Data obtained in 3 experiments, n=8–9 oocytes per group per experiment.

(B) Western blot showing phosphorylation levels of eIF2α from untreated oocytes, oocytes treated for 2 hrs with 2.5 μg/ml Tn, or Vh, and Tn + Em. Actin western blots are shown as loading control. For (B), (D) and (F), two oocyte equivalents were loaded per lane and proteins were resolved through 12% SDSPAGE. In (B), these gels represent 4 independent western blots with n=15–20 oocytes per group.

(C) Histograms of the ratio of P-eIF2α normalized with actin are represented as the mean ± SEM.

(D) Western blot showing protein levels of BiP from untreated oocytes (C), oocytes treated with Tn, and oocytes treated with Tn + Em. These gels represent 3 independent western blots with n=10 oocytes per group.

(E) Histograms of the ratio of BiP normalized with actin are represented as the mean ± SEM. Asterisks indicate statistical significance (*$p<0.05$, **$p<0.001$, ANOVA).